

## Kinetics of phase ordering with topological textures

Martin Zapotocky\*

*Department of Physics and Materials Research Laboratory,  
University of Illinois at Urbana-Champaign, Urbana, Illinois 61801*

Wojtek Zakrzewski†

*Department of Mathematical Sciences, University of Durham, Durham DH1 3LE, United Kingdom*

(Received 1 February 1995)

We study the role played by topological textures and antitextures during the phase ordering of a two-dimensional system described by the discretized nonlinear  $O(3)$   $\sigma$  model with purely dissipative dynamics. We identify and characterize two distinct mechanisms for the decay of the order parameter variations—single texture unwinding, and topological charge annihilation. Our results show that, while at early times after the quench, the annihilation process dominates, the unwinding processes become of comparable importance at later times. We calculate the correlations in the order parameter and in the topological charge density, and show that dynamical scaling is strongly violated due to the occurrence of multiple length scales growing differently in time.

PACS number(s): 64.60.Cn, 82.20.Mj, 05.70.Fh, 11.27.+d

The field of phase-ordering kinetics, investigating the time evolution of a system quenched from the disordered phase into the ordered phase, has attracted considerable attention in recent years [1]. It has been shown that many features of phase ordering in systems supporting topologically stable singular defects [for example, in systems described by the  $O(N)$  vector model in  $d$  spatial dimensions with  $d \geq N$  [2], or in two- and three-dimensional nematic liquid crystals [3]] can be understood theoretically by investigating the dynamics of the numerous topological defects generated during the quench. In systems where topologically stable singular objects cannot occur [for example, in the  $O(N)$  model system in dimension  $d < N$ ], such an approach cannot be used. A special and interesting case is that of the  $O(N)$  model system in  $N-1$  spatial dimensions, which supports topologically stable, but nonsingular objects—topological textures. The purpose of this paper is to report results from an investigation of the role played by topological textures during the phase ordering of an  $O(3)$  vector model system in two spatial dimensions. This system has been previously investigated by Toyoki [4], who calculated the time dependence of the order parameter correlation function, and by Bray and Humayun [5], who investigated the decay of the free energy in the system. A detailed analysis of the phase-ordering process in terms of the behavior of the topological objects present in this system, however, has not been previously given [6].

The model investigated in our simulations is the nonlinear  $O(3)$   $\sigma$  model on a two-dimensional lattice. The order parameter  $\mathbf{m}$  is correspondingly a three-component vector with unit magnitude; the local value of the order parameter  $\mathbf{m}(\mathbf{r}, t)$  will be referred to as the spin. The phase-ordering simulation is started with randomly oriented spins, corresponding to the configuration generated immediately after a

quench to zero temperature. The configuration is then evolved using the dissipative dynamical equation

$$\frac{\partial \mathbf{m}}{\partial t} = \nabla^2 \mathbf{m} - (\mathbf{m} \cdot \nabla^2 \mathbf{m}) \mathbf{m}, \quad (1)$$

where the second term on the right hand side enforces the constraint  $\mathbf{m} \cdot \mathbf{m} = 1$ . To adequately describe the phase-ordering process, Eq. (1) must be regularized on a scale given by the equilibrium bulk correlation length; we effectively impose the regularization condition by considering Eq. (1) on a discrete lattice. We evolved Eq. (1) using the technique developed in Ref. [7] (based on the fourth order Runge-Kutta method) appropriately adapted to our case. The spatial discretization step was taken to be  $dx = dy = 0.1$ , the time step was  $dt = 0.0002$ , and we worked with periodic boundary conditions. We used system sizes between 252 and 512 lattice units, and our longest runs reached times  $t = 40$ .

We now briefly review the concept of a topological texture [8]. The spin configuration of an example of a single texture in an infinite continuum system is given by

$$m_x(\mathbf{r}) = \frac{4ax}{r^2 + 4a^2}, \quad m_y(\mathbf{r}) = \frac{4ay}{r^2 + 4a^2}, \\ m_z(\mathbf{r}) = \frac{r^2 - 4a^2}{r^2 + 4a^2}. \quad (2)$$

The orientation of the spin changes from up in the center of the texture ( $r=0$ ) to down at the boundary of the system ( $r=\infty$ ), going through a vortexlike configuration with spins pointing radially outwards on the circle  $r=2a$ . It is easily seen that the spin configuration (2) covers the order parameter space (given in our case by the unit sphere in three dimensions) exactly once, corresponding to a topological charge of 1. It is possible to show that the configuration (2) (or any global rotation thereof) has the minimum energy [with energy density taken as  $(1/8\pi)(\nabla \mathbf{m})^2$ ] of all configura-

\*Electronic address: zapotock@uiuc.edu

†Electronic address: w.j.zakrzewski@durham.ac.uk

rations with topological charge 1. The value of the minimum total energy is  $E = 1$ . By an *antitexture*, we mean a configuration similar to (2), but with  $m_y(\mathbf{r})$  replaced by  $-m_y(\mathbf{r})$ . This configuration wraps around the spin sphere once, but in the opposite sense compared to (2), corresponding to topological charge  $-1$ .

The crucial quantity for our investigation of the role of textures and antitextures in the phase ordering process is the *topological charge density*  $q(\mathbf{r})$

$$q(\mathbf{r}) = \frac{1}{4\pi} \mathbf{m} \cdot (\partial_x \mathbf{m} \times \partial_y \mathbf{m}) \quad (3)$$

which, when integrated over the whole system, gives the total topological charge. For the single texture configuration (2), the topological charge density has the form  $q(r) = (1/\pi)4a^2/(r^2 + 4a^2)^2$ , and exhibits a pronounced peak at  $r=0$  with half-width  $1.287a$ . For a single antitexture,  $q(r)$  is of the same form, only negative.

In Figs. 1(a)–1(c), we plot the topological charge density at a progressive series of times in a section of a system undergoing phase ordering. The plots exhibit numerous well defined peaks and antipeaks, corresponding at later times to rather well separated textures and antitextures of varying sizes. The average separation between the textures (or antitextures) grows, and at the latest time, the system is strongly “intermittent” in the sense that the topological charge density differs significantly from zero only within very well localized regions, with the spin configuration practically homogeneous in between. Note that the “typical” texture size does not appreciably increase with time.

A detailed inspection of series of plots similar to Fig. 1, taken at more closely spaced values of time, reveals that the variations in topological charge density decay through two distinct processes: single texture (or antitexture) unwinding, and topological charge annihilation. The first process appears as a growing isolated peak in topological charge density, and corresponds to a localized configuration of type (2) with decreasing size  $a$ . Such a process would conserve the total topological charge and the total energy of the texture in a continuum system; in a discrete system, however, this conservation is strongly violated once the texture size decreases to several lattice spacings. Eventually, the texture comes (up to a global rotation) close to the extreme configuration where the spin points up at the center lattice point, and down everywhere else; such a configuration has only  $1/2\pi$  of the original texture energy. This configuration is followed by a flip of the central spin, and the complete disappearance of the texture [9]. The size  $a$  of the shrinking texture in our simulation varied very roughly as  $\tau^{1/4}$ , where  $\tau$  is the time remaining to the flip.

The second process visible in the topological charge density plots is the mutual annihilation of overlapping regions of positive and negative topological charge density [overlapping in the sense that they are not separated by a region where  $q(\mathbf{r})=0$ ]. In Fig. 2, we show the evolution starting from a slightly overlapping texture-antitexture pair. The height of the two peaks decays, and the overlap of the regions of positive and negative  $q(\mathbf{r})$  increases with time. The peaks initially move slightly together, but later move significantly apart [10]. It is important to realize that this “texture-

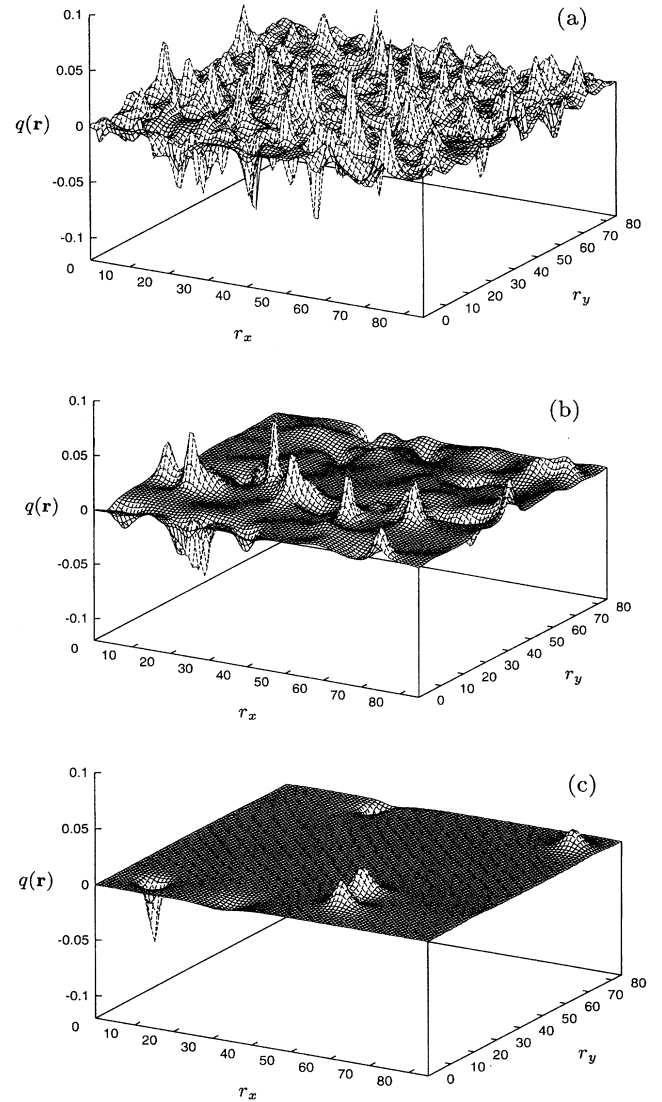


FIG. 1. Surface plots of the topological charge density  $q(\mathbf{r})$  in an  $85 \times 85$  section of a phase-ordering system at time (a)  $t = 0.0356$ , (b)  $t = 0.126$ , and (c)  $t = 1.59$ . The horizontal scale is in units of one lattice spacing.

antitexture annihilation” process differs radically from the process of annihilation of a singular defect with its antidefect [e.g., a vortex and an antivortex in the two-dimensional  $O(2)$  model], where the singular cores keep their identities and gradually approach. In the texture-antitexture annihilation, the total charge enclosed by each of the regions of positive and negative  $q(\mathbf{r})$  gradually decays to zero, and the annihilation of topological charge occurs independently of whether a complete texture and antitexture are present. In contrast to this, the mechanism of unwinding (discussed in the preceding paragraph) occurs only if the unwinding region encloses a total topological charge close to 1 or  $-1$ .

In order to assess the relative importance of the two processes discussed above during phase ordering, we investigated the time dependence of the quantities  $Q_+$  and  $Q_-$ , defined by

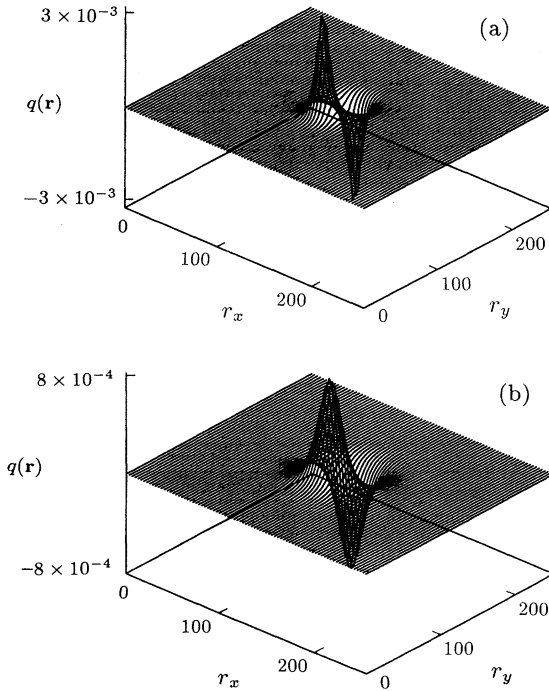


FIG. 2. The process of topological charge annihilation, starting from an overlapping full texture and antitexture. The plots show  $q(\mathbf{r})$  for (a)  $t=0$  (initial configuration) and (b)  $t=3.0$ . Note that the vertical scale is different in (a) and (b). The quantity  $P = \int d^2r |q(\mathbf{r})|$  decays from 1.54 in (a) to 0.89 in (b).

$$Q_+ = \int d^2r \max[q(\mathbf{r}), 0], \quad Q_- = \int d^2r \min[q(\mathbf{r}), 0], \quad (4)$$

where the integral is over the whole system. In a system with well separated textures and antitextures,  $Q_+$  counts the number of textures,  $Q_-$  counts the number of antitextures,  $Q = Q_+ + Q_-$  gives the total topological charge, and  $P = Q_+ - Q_-$  counts the total number of topological objects in the system. Figure 3 shows that, at late times, the total

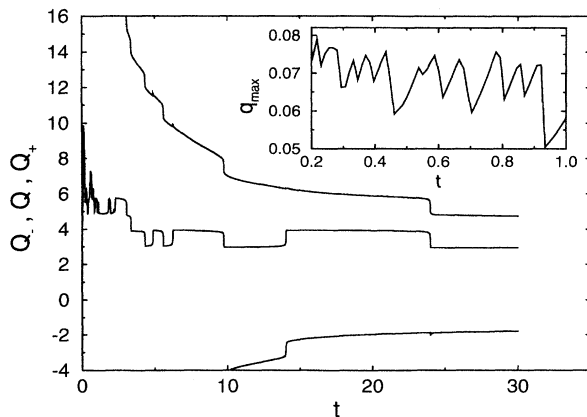


FIG. 3. Time dependences of the quantities  $Q_-(t)$  (lower curve),  $Q(t)$  (middle curve), and  $Q_+(t)$  (upper curve) during phase ordering of a system of size  $252 \times 252$ . Inset: time dependence of  $q_{\max}(t)$ .

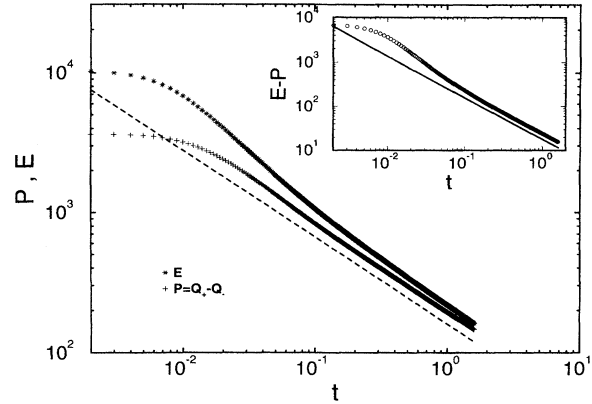


FIG. 4. Time dependences of the integrated absolute charge  $P(t)$  and the free energy  $E(t) = \int d^2r (1/8\pi)(\nabla \mathbf{m})^2$  during phase ordering of a system of size  $512 \times 512$ , averaged over 14 initial conditions. The dashed line has a slope of  $-0.64$ . Inset: the decay of the difference  $E(t) - P(t)$ . The full line has a slope of  $-0.92$ .

topological charge  $Q = Q_+ + Q_-$  varies only in sharp steps of size  $-1$  ( $+1$ ), corresponding to an unwinding of a single texture (antitexture). The steps are also visible in the corresponding  $Q_+(t)$  or  $Q_-(t)$  curve (see Fig. 3). Note, however, that while the  $Q(t)$  curve is flat, the  $Q_+(t)$  and  $Q_-(t)$  curves decay significantly in between the unwinding steps. This demonstrates that the process of topological charge annihilation, as defined earlier, takes place. The relative importance of the unwinding and annihilation processes in a given time range is given by the ratio of the number of steps in the  $Q(t)$  curve to the total drop of the integrated absolute topological charge density  $P = Q_+ - Q_-$ . In the time interval between  $t=3$  and  $t=30$ , this ratio is  $\rho = 0.45$ , showing that in this time range, unwindings and the annihilation processes play almost equally important roles. At earlier times, it is difficult to calculate the ratio  $\rho$ , as the total topological charge  $Q$  of a large system no longer exhibits well separated steps. A lower bound for  $\rho$ , however, may still be obtained by counting the sharp peaks (see the inset in Fig. 3) occurring in the curve  $q_{\max}(t)$ , where  $q_{\max}$  is defined as the maximum of  $|q(\mathbf{r})|$  over the whole system. Each peak corresponds to the final stages of shrinking and consequent flipping of a texture or antitexture; however, if two textures unwind at almost the same time in two different parts of the system, only one peak may be visible. Comparing the number of peaks with the drop in  $P(t)$  in the time interval from  $t=0.5$  to  $t=1.0$  gives  $\rho \geq 0.25$ . This is consistent with the expectation that since the textures and antitextures are better separated as  $t$  increases (see Fig. 1),  $\rho$  should increase with time.

We now present results averaged over 14 runs in a system of size 512, evolved until  $t=1.6$ . Longer runs in systems of size 252 gave similar results. The total topological charge  $Q$  was approximately conserved and close to zero [ $|Q(t)| < 5$  at all  $t$ ]. In Fig. 4, we plot the integrated absolute charge  $P = Q_+ - Q_-$ , the free energy  $E$ , and their difference. The asymptotic equality of  $E$  and  $P$  indicates that, at late times, the system is well separated into textures and antitextures, each of energy 1. Note that the inequality  $E(t) > P(t)$  is satisfied at all times; this is consistent with the well known

[11] global inequality  $E \geq |Q|$  being valid inside each region containing a texture or an antitexture [12]. Both  $P$  and  $E$  decay asymptotically as  $t^{-0.64 \pm 0.02}$ , indicating that the average separation  $D(t)$  between topological objects (textures or antitextures) grows as  $t^{0.32 \pm 0.01}$ . Note that this differs significantly from the dimensional analysis prediction of a length scale growing as  $t^{1/2}$ , and points towards the presence of scaling violations. In contrast, the difference  $E(t) - P(t)$ , characterizing topologically trivial spin variations, decays asymptotically as  $t^{-0.92 \pm 0.03}$  (see the inset in Fig. 4) which agrees much better with the dimensional analysis result. The onset of the approximate power-law regime for  $P(t)$  occurs at  $t \approx 0.02$ , corresponding to the time after which well formed textures and antitextures are seen in the topological charge density plots.

We calculated three separate correlation functions: the spin-spin correlation  $C(r, t) = \langle \mathbf{m}(\mathbf{x}) \cdot \mathbf{m}(\mathbf{x} + \mathbf{r}) \rangle$ , the topological charge density correlation  $C_q(r, t) = \langle q(\mathbf{x})q(\mathbf{x} + \mathbf{r}) \rangle / \langle q(\mathbf{x})q(\mathbf{x}) \rangle$ , and the correlation of the absolute topological charge density,  $C_p(r, t) = \langle p(\mathbf{x})p(\mathbf{x} + \mathbf{r}) \rangle / \langle p(\mathbf{x})p(\mathbf{x}) \rangle$  [here  $p(\mathbf{x}) = |q(\mathbf{x})| - \langle |q| \rangle$ , and  $\langle \rangle$  denotes averaging over the whole system]. We define the length scales  $L(t)$ ,  $L_q(t)$ , and  $L_p(t)$  as the half-widths of the central maxima of the correlation functions  $C(r, t)$ ,  $C_q(r, t)$ , and  $C_p(r, t)$ , respectively. We find that these length scales grow differently from each other (see the inset in Fig. 5) and from the average separation of topological objects  $D(t)$ , indicating that dynamical scaling is violated. The half-widths  $L_q(t)$  and  $L_p(t)$  do not grow as power laws of time, but rather as  $a \log(bt)$ , where  $a$  and  $b$  are constants. The half-width of the spin-spin correlation,  $L(t)$ , grows much faster, and at late times fits the power law  $L(t) \propto t^{0.38 \pm 0.02}$  [13].

We furthermore find that each family of the correlation functions individually does not collapse onto a universal curve, providing a further indication of the violation of dynamical scaling. In Fig. 5, we show an attempt to collapse the correlation functions  $C(r, t)$ ,  $C_q(r, t)$ , and  $C_p(r, t)$  using the lengths  $L(t)$ ,  $L_q(t)$ , and  $L_p(t)$ . The lack of collapse is

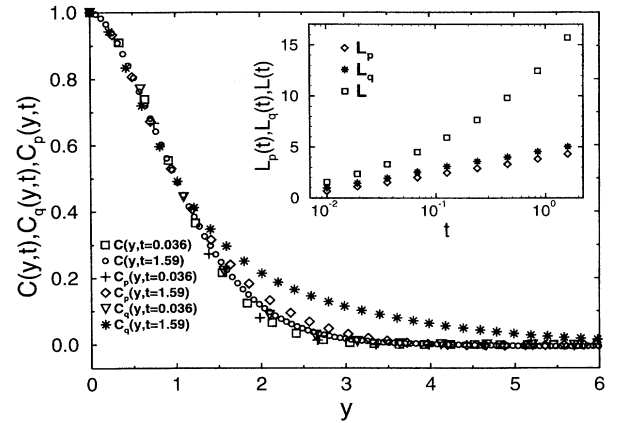


FIG. 5. The rescaled correlation functions  $C(r/L(t))$ ,  $C_q(r/L_q(t))$ , and  $C_p(r/L_p(t))$  at specified times (see the main text for definitions). Inset: growth of the length scales  $L(t)$ ,  $L_q(t)$ , and  $L_p(t)$  (note that the graph is semilogarithmic).

most readily apparent in the topological charge correlation  $C_q(r, t)$ . A more detailed discussion of our results for the topological correlation functions will be given separately.

In conclusion, we have characterized the phase-ordering kinetics in the investigated system in terms of the distinct processes of single texture unwindings and topological charge annihilation, and demonstrated that dynamical scaling is strongly violated. Most of the methods developed in this paper should be equally well applicable to phase ordering in systems with topological textures in higher dimensions.

We thank J. Borrill, A. J. Bray, N. Goldenfeld, and Y. Oono for useful discussions, and the Isaac Newton Institute, where this collaboration was started, for hospitality. M.Z. acknowledges support by the U.S. National Science Foundation through Grants No. NSF-DMR-89-20538 and No. NSF-DMR-94-24511.

- [1] For a recent review of the theory of phase ordering, see A. J. Bray, *Adv. Phys.* **43**, 357 (1994).
- [2] A. J. Bray and K. Humayun, *Phys. Rev. E* **47**, 9 (1993); B. Yurke *et al.*, *ibid.* **47**, 1525 (1993).
- [3] M. Zapotocky, P. M. Goldbart, and N. Goldenfeld, *Phys. Rev. E* **51**, 1216 (1995); M. Zapotocky and P. M. Goldbart (unpublished).
- [4] H. Toyoki, *Mod. Phys. Lett. B* **7**, 397 (1993).
- [5] A. J. Bray and K. Humayun, *J. Phys. A* **23**, 5897 (1990).
- [6] We recently received a preprint by A. J. Rutenberg (Report No. cond-mat/9501071), who has independently investigated phase ordering in the Heisenberg model in two dimensions. Although the emphasis of the two articles is somewhat different, our numerical results agree where the two papers overlap.
- [7] R. A. Leese, M. Peyrard, and W. J. Zakrzewski, *Nonlinearity* **3**, 387 (1990).
- [8] See, e.g., R. Rajaraman, *Solitons and Instantons* (North-Holland, Amsterdam, 1982).

- [9] The unwinding process occurs somewhat differently – through the reduction of the order parameter magnitude in the center of the texture – in the “soft-spin” continuum  $O(N)$  vector model. In both the discrete nonlinear  $\sigma$  model and the continuum “soft-spin” model, however, the texture disappears once it reaches a certain *finite* radius.
- [10] Details of our investigation of the annihilation process will be reported separately.
- [11] A. A. Belavin and A. M. Polyakov, *Pis'ma Zh. Eksp. Teor. Fiz.* **22**, 503 (1975) [*JETP Lett.* **22**, 245 (1975)].
- [12] Neighboring regions with small amounts of positive and negative topological charge, undergoing annihilation, can have  $E$  substantially larger than  $P$  [10]. However, the contribution of such regions to the total values of  $E$  and  $P$  in the whole system is small.
- [13] This is roughly consistent with the result  $L(t) \propto t^{0.42 \pm 0.03}$  in [4].